

Electrochemical Behavior of 3,4-ethylenedioxythiophene as an Anti-overcharge Additive for Lithium-ion Batteries

Sai Wang¹, Jianxiong Liu¹, Xiaohua Yu^{1,*}, Jiaming Liu³, JuRong¹, Chengyi Zhu¹, Qiang Wang¹, Zhentao Yuan¹, Yannan Zhang^{2,*}

¹ Faculty of Materials Science and Engineering, Kunming University of Science and Technology, Kunming 650093, China

² National and Local Joint Engineering Laboratory for Lithium-ion Batteries and Materials Preparation Technology, Key Laboratory of Advanced Battery Materials of Yunnan Province, Faculty of Metallurgical and Energy Engineering, Kunming University of Science and Technology, Kunming 650093, China

³ School of Metallurgy Engineering, Jiangxi University of Science and Technology, Ganzhou 341000, China

*E-mail: xiaohua_y@163.com (Xiaohua Yu), zyn_legolas@163.com (Yannan Zhang)

Received: 5 June 2019 / Accepted: 28 July 2019 / Published: 30 August 2019

The overcharge protection performance of $\text{LiNi}_{0.8}\text{Co}_{0.1}\text{Mn}_{0.1}\text{O}_2$ as the positive electrode materials for the lithium-ion batteries is significantly enhanced by adding 3,4-ethylenedioxythiophene (EDOT) into the electrolyte. The effect of anti-overcharge on $\text{LiNi}_{0.8}\text{Co}_{0.1}\text{Mn}_{0.1}\text{O}_2$ electrodes are analyzed by microelectrode linear scan voltammetry measurement, electrochemical impedance measurement, constant current charge/discharge and overcharged tests. The cycled electrodes are also tested by scanning electron microscopy (SEM) and X-ray diffraction (XRD) analysis. The results show that the EDOT additive can react with the base electrolyte and easily form a polymer layer on the surface of $\text{LiNi}_{0.8}\text{Co}_{0.1}\text{Mn}_{0.1}\text{O}_2$ electrodes at a stable platform of 4.4 V (vs Li/Li⁺). The time for the voltage rising to the overcharge state is apparently delayed from 25 h to 58 h. After 100 cycles at 0.5 C rate, the capacity retention rate of the half-cell is increased from 80.1% to 93.4% after adding the EDOT additive. The results demonstrate that this promising anti-overcharged and cyclic performance are attributed to the protective film generated by EDOT which may enhance the interfacial stability of $\text{LiNi}_{0.8}\text{Co}_{0.1}\text{Mn}_{0.1}\text{O}_2$ /electrolyte.

Keywords: 3,4-ethoxylenedioxythiophene, electrolyte additive, overcharge, $\text{LiNi}_{0.8}\text{Co}_{0.1}\text{Mn}_{0.1}\text{O}_2$, lithium-ion batteries

1. INTRODUCTION

Lithium-ion batteries (LIBs) have been widely applied in all kinds of devices ranging from portable electronic devices to electric vehicles (EVs), as well as large-scale energy storage systems [1-

3]. In order to meet the growing demand for energy density, $\text{LiNi}_{0.8}\text{Co}_{0.1}\text{Mn}_{0.1}\text{O}_2$ as the positive electrode materials have received extensively attention due to its promising theoretical capacity [4-7]. However, the electrolytes are prone to undergoing the decomposition and further form some lithium dendrites under high voltage and overcharge conditions, which may lead to leakage and explosion and cannot meet the demand for the fast-developing electric vehicles [8,9]. In order to solve this problem, Some the anti-overcharged additives are introduced to the electrolyte by preventing the excessive redox and electro-polymerization reaction. When the voltage continues to rise, the additive could inhibit the oxidative decomposition of the electrolyte. This internal protection mechanism can effectively improve the safety of lithium-ion batteries [10-13]. For example, aromatic compounds such as alkyl 3,3,3-trifluoropropanoate [14] and 4-bromoanisole [15] are used as anti-overcharge additives, which can preferentially form a stable film covering the surface of the electrodes, and finally restrain the increasing of internal voltage.

Therefore, some efforts have been made to explore suitable electrolyte additives for the high energy density lithium-ion batteries under extreme working condition. Xiao et al. introduced biphenyl as an anti-overcharged electrolyte additive, and discovered that a conductive film is formed on the surface of positive materials attribute to the electro-polymerization reaction in 4.5 V, which is effective to restraining overcharge behaviors [16]. Zhao et al. discovered that the electrolyte with methyl benzenesulfonate (MBS) can form a group of faults when the voltage of the cell exceeds the MBS electro polymerization potential, thereby preventing the further decomposition of the electrolyte and effectively improving the safety of the lithium-ion batteries [17]. It has been reported that 3,4-ethylenedioxythiophene (EDOT) can be directly used as an electrolyte additive for LiCoO_2 lithium-ion batteries, which can significantly improve its cyclic stability under extreme working condition [18,19]. However, the impact on the safety performance of Ni-rich positive materials of lithium-ion batteries have not been studied. Herein, we have directly introduced EDOT as the functional electrolyte additive for the Ni-rich positive materials. Its electro-polymerization behavior on the anti-overcharge and cyclic performance of lithium ion battery are detailedly explored.

2. EXPERIMENTAL

2.1 Preparation of electrolytes and electrodes

The electrochemical properties of different electrolytes were investigated through the CR2032-type coin cells, consisting of $\text{LiNi}_{0.8}\text{Co}_{0.1}\text{Mn}_{0.1}\text{O}_2$ as a working electrode, lithium foil as a counter electrode. The blank electrolyte solution was 1 mol L^{-1} LiPF_6 in a mixed solvent of ethylene carbonate (EC)/ethyl methyl carbonate (EMC) (in a volume ratio of 3:7). 0.5 wt.%, 1.0 wt.%, 2.0 wt.% EDOT was added to obtain the EDOT containing electrolyte, and named as E1, E2, and E3, respectively. The electrolyte was mixed in a vacuum drying oven. The water and free acid (HF) contents in the electrolyte were kept below 20 and 50 ppm, respectively $\text{LiNi}_{0.8}\text{Co}_{0.1}\text{Mn}_{0.1}\text{O}_2$ (Hunan Shanshan Toda Advanced Materials Co., Ltd) was selected as the active electrode materials. The positive electrodes were prepared with a slurry of 80 wt.% $\text{LiNi}_{0.8}\text{Co}_{0.1}\text{Mn}_{0.1}\text{O}_2$ powders, 10 wt.% polyvinylidene fluoride (PVDF) and 10 wt.% acetylene black binder in N-methyl-2-pyrrolidone (NMP). The slurry was cast on aluminum foil

to prepare working electrodes. Finally, the CR2032-type coin cells were assembled in a glove box filled with Ar (MIKROUNA Universal (2440/750/900)).

2.2 Electrochemical measurement

The electrochemical behavior of electrolyte with or without EDOT was studied by microelectrode linear sweep voltammetry (LSV) through an electrochemical workstation (CHI660C, China). LSV was performed in a three-electrode cell using Pt as working electrode, a Li metal as counter and reference electrodes with a scan rate of 0.1 mV s^{-1} . The charge and discharge test system (Land CT2001A, China) was used to conduct constant current measurement and overcharge test. Firstly, the battery was conducted with the voltage range of 2.8-4.2 V at the current density of 0.2 C for 3 cycles, then charge/discharge process was performed at a constant current density of 0.2 C and a cut-off voltage of 5 V.

The electrochemical impedance spectroscopy (EIS) of as prepared samples were also tested by the same electrochemical workstation (CHI660C, China) before and after overcharging. The frequency range from 100 kHz to 10 mHz with an amplitude of 5 mV. In order to evaluate the influence of EDOT on cycle performance, charge-discharge measurements were conducted by Land CT-2001A battery tester with the voltage range of 2.8-4.7 V at 0.5 C.

2.3 Morphology and structural characterization

The overcharged coin cells were disassembled in an argon-filled glovebox. The $\text{LiNi}_{0.8}\text{Co}_{0.1}\text{Mn}_{0.1}\text{O}_2$ positive materials were rinsed with high-purity dimethyl carbonate (DMC) to remove residual electrolyte, and then dried in a vacuum oven at 60°C for 12 h. The surface morphology of the electrodes before and after overcharging were analyzed by scanning electron microscopy (TESCAN VEGA3 SBH).

3. RESULTS AND DISCUSSION

3.1 Electro-polymerization behavior of EDOT

Fig. 1 shows the linear scanning curves of $\text{LiNi}_{0.8}\text{Co}_{0.1}\text{Mn}_{0.1}\text{O}_2$ working electrode with a three-electrode cell indifferent electrolyte solutions. In the blank electrolyte, the oxidation current is increased when the voltage is rising up to 4.2 V, which is caused by the oxidation reaction of the electrolyte on the platinum electrode. However, the scanning curves in the electrolyte with different content of EDOT exhibit significantly different. The oxidation currents are increased rapidly with the voltage rising when the working potential is close to 4.0 V. Finally, the oxidation currents are reached the maximum at 4.4 V. This is because that the EDOT adsorbs on the Pt electrode will undergo an electrolyte oxidation reaction and generate a weak current. Furthermore, a large amount of EDOT in the electrolyte undergo an oxidation reaction and the current will rise sharply at high voltage state. This process is controlled by the diffusion of EDOT in the electrolyte [14]. The linear scan curves indicate that EDOT has a suitable oxidation potential as an overcharge protection additive for Ni-rich positive materials.

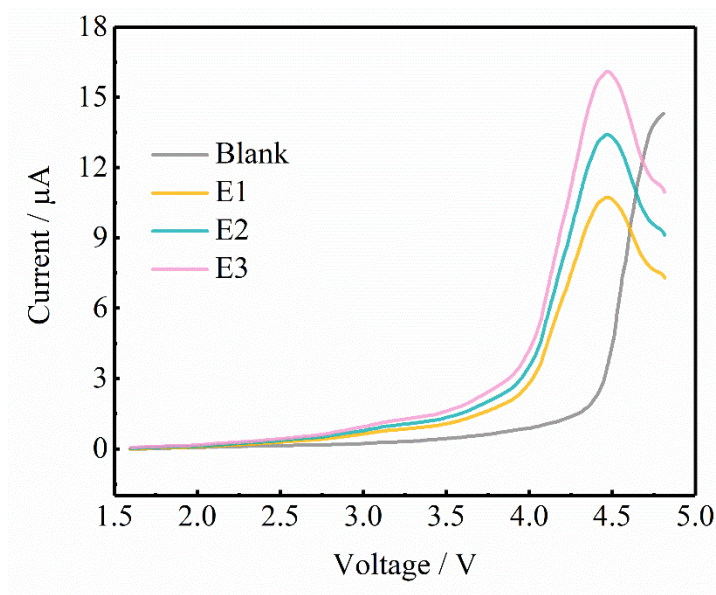


Figure 1. Potentiodynamic polarization curves of Pt microelectrode in $1 \text{ mol}\cdot\text{L}^{-1}$ $\text{LiPF}_6/\text{EC}/\text{DMC}$ with or without EDOT at sweep rate $0.1 \text{ mV}\cdot\text{s}^{-1}$.

Fig. 2 plots the CV curves of four different samples at a scan rate of $0.5 \text{ mV}\cdot\text{s}^{-1}$. It can be clearly seen that the blank sample exhibits a pair of redox peaks appear in the range of 2.8-3.2 V, which corresponds to the reversible Li^+ intercalation and desorption reaction of the blank sample [5, 20], which also exhibits an oxidation peak at a voltage of 4.5 V. Compared with the blank one, the CV curves of other three samples also show a pair of redox peaks in the range of 2.8-3.2 V, respectively, indicating that the addition of EDOT does not influence the electrochemical performance of $\text{LiNi}_{0.8}\text{Co}_{0.1}\text{Mn}_{0.1}\text{O}_2$ electrodes. In addition, the significant oxidation peaks are observed at 4.4 V, corresponding to the oxidation reaction of the EDOT and the electrodes. This results indicates that the sacrificial oxidation of the EDOT additive on the cathode surface can easily generate a protective film at high voltage state.

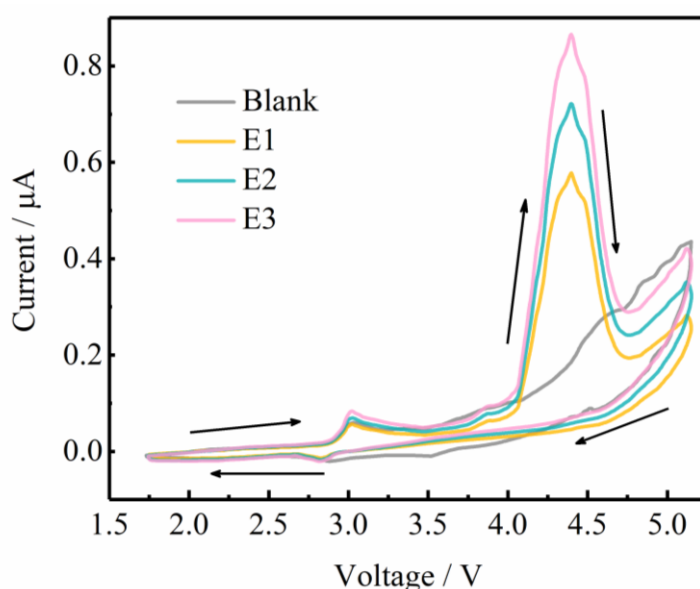


Figure 2. CV curves of $\text{LiNi}_{0.8}\text{Co}_{0.1}\text{Mn}_{0.1}\text{O}_2$ microelectrode in $1 \text{ mol}\cdot\text{L}^{-1}$ $\text{LiPF}_6/\text{EC}/\text{DMC}$ with or without different content EDOT, scan rate $0.5 \text{ mV}\cdot\text{s}^{-1}$.

3.2 The effect of EDOT on the overcharge performance of the battery.

To evaluate the effect of EDOT on the overcharge behavior of $\text{LiNi}_{0.8}\text{Co}_{0.1}\text{Mn}_{0.1}\text{O}_2$ lithium ion batteries, the galvanostatic charge and discharge experiments was conducted. The half-cells were first cycled thrice between 2.7-4.2 V at 0.2 C, and then charged to 5 V at the same rate. It can be seen in Fig. 3 that the U-t curves are nearly overlapped when the as prepared four samples with different EDOT-containing are cycled in the range between 2.7-4.2 V, indicating that the EDOT does not apparently affect the transportation of Li-ions under the 4.2 V. However, the U-t curves of four samples begins to change when the applied voltage is greater than 4.2 V after three cycles, the charging voltage of blank sample rapidly rises up to 5 V. In contrast, the potentials of other three samples containing EDOT rise slowly (Fig.3c-d). Notably, there is a stable platform appears and the voltage does not increase after reaching 4.4 V when the additive content is upto 2.0 wt.%. This can be ascribed to the decomposition of EDOT at 4.4 V and the subsequent oxidation products formation on the surface of the positive electrode, which also may increase the resistance of the positive materials, thereby suppressing the voltage rise and improving the safety performance of the battery. As can be seen from Fig. 3, as the EDOT content is upto 1.0 wt.%, the voltage platform can be effectively prolonged.

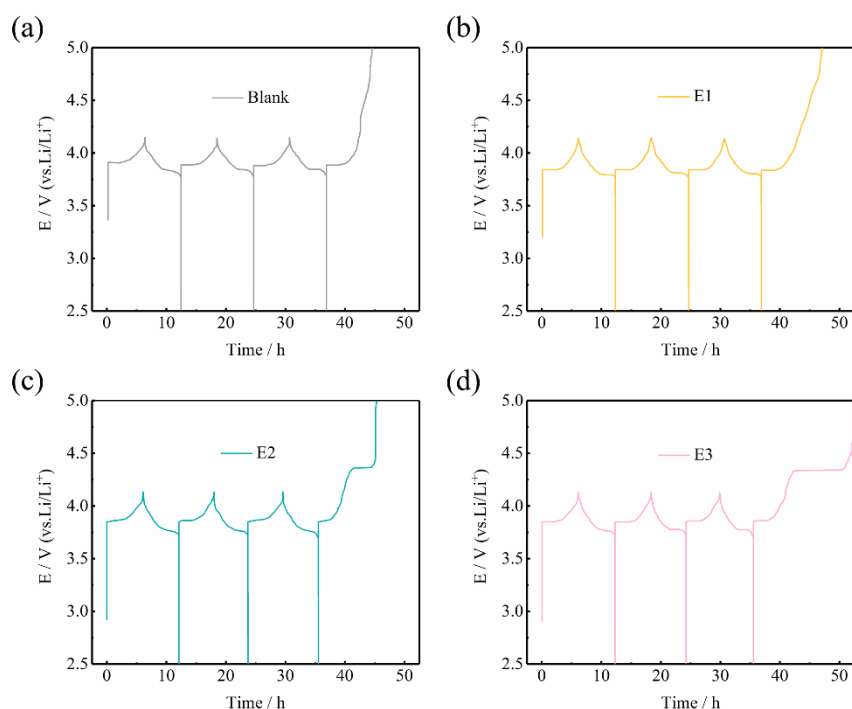


Figure 3. U-t curves of the $\text{LiNi}_{0.8}\text{Co}_{0.1}\text{Mn}_{0.1}\text{O}_2/\text{Li}$ half-cells during charge/discharge and overcharged curves for four samples, respectively.

3.3 Electrochemical impedance spectroscopy

The improvement in anti-overcharged performance can be explained by the increase in the impedance of the batteries after overcharge. The Nyquist plots and fitted value curves with different EDOT-containing are shown in Fig. 4 (the inset in Fig. 4 is the equivalent circuit model diagram). It can be clearly seen that each of the plots consists of a semicircle in high-medium frequency region, which

presents charge transfer impedance (R_{ct}). The oblique line in the low-frequency region is assigned to Warburg impedance of lithium ions transferred in the electrode active materials [21,22]. After overcharging, the electrolyte resistance (R_s) of the four as-prepared samples are increased from 1.4 Ω , 1.7 Ω , 3.6 Ω , and 4 Ω to 5.9 Ω , 6.8 Ω , 8.5 Ω , and 11.6 Ω , respectively. The R_{ct} of the blank electrolyte sample is not significantly changed. By comparison, the R_{ct} of the samples containing the EDOT additive are obviously increased from 162 Ω , 315 Ω , and 386 Ω to 386 Ω , 508 Ω , and 612 Ω , respectively. It is because the sacrificial oxidation of the EDOT additive on the surface of the positive materials can effectively hinder the charge transfer under overcharge conditions. This result further supports the previous conclusions of the overcharge test.

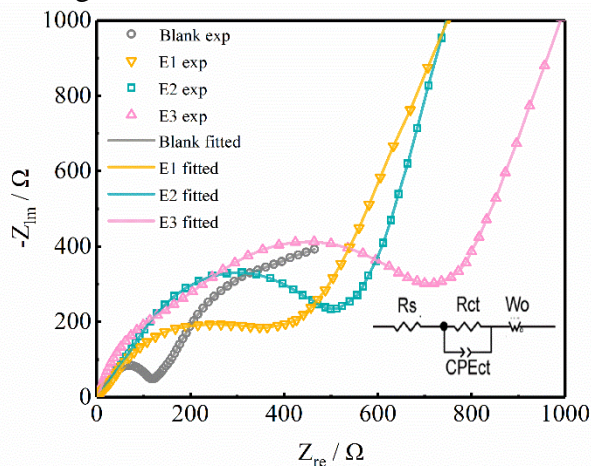


Figure 4. Nyquist plots and equivalent circuit model of $\text{LiNi}_{0.8}\text{Co}_{0.1}\text{Mn}_{0.1}\text{O}_2/\text{Li}$ half-cells overcharged with different mass ratio EDOT electrolyte.

Table 1. Fitting circuit parameters of $\text{LiNi}_{0.8}\text{Co}_{0.1}\text{Mn}_{0.1}\text{O}_2/\text{Li}$ half-cells.

Samples	Blank		E1		E2		E3	
	R_s	R_{ct}	R_s	R_{ct}	R_s	R_{ct}	R_s	R_{ct}
Overcharge before	1.4	156	1.7	162	3.6	315	4.0	386
Overcharge after	6.0	232	7.0	386	9	508	12	612

3.4 Effect of EDOT on electrochemical performance of $\text{LiNi}_{0.8}\text{Co}_{0.1}\text{Mn}_{0.1}\text{O}_2$

Fig. 5 shows the cycling performance of the four as-prepared samples with different content of EDOT additive at a high cut-off voltage of 4.7 V. The discharge specific capacity of the blank electrolyte is decreased from the initial 185.38 mAh g^{-1} to 148.57 mAh g^{-1} . The capacity retention was only 80.1% after 100 cycles. By comparison, after adding the EDOT additives, the capacity retention of other three samples (E1, E2 and E3) are reached upto 90.2%, 93.4% and 90.0%, respectively, which are significantly higher than that of the blank one. The improvement of the cycling stability is due to the sacrificial oxidation of the EDOT additive on the electrode surface to generate a passivation film, which restrains the electrolyte oxidation and crystal structural damage [18, 23-26]. The schematic diagram of the action

process is shown in Fig. 6. The capacity retention of 2.0 wt.% EDOT is lower than that of the 1.0 wt.% EDOT, indicating that the EDOT concentration is not favorite as high as possible, this is because the excessive additive may hinder the migration of Li^+ , and the extra Li ions are easily deposited on the surface of the negative electrode, resulting in capacity decay [27].

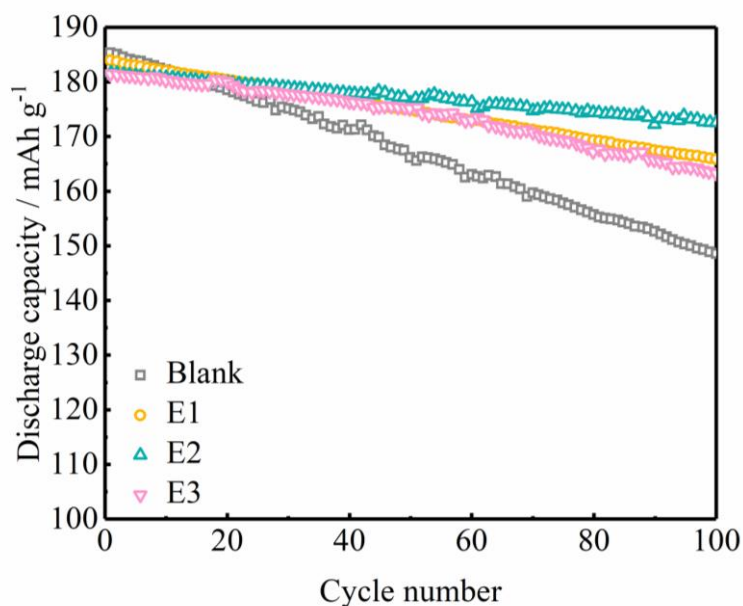


Figure 5. Cyclic performance of different samples: (a) Blank, (b) E1, (c) E2, (d) E3.

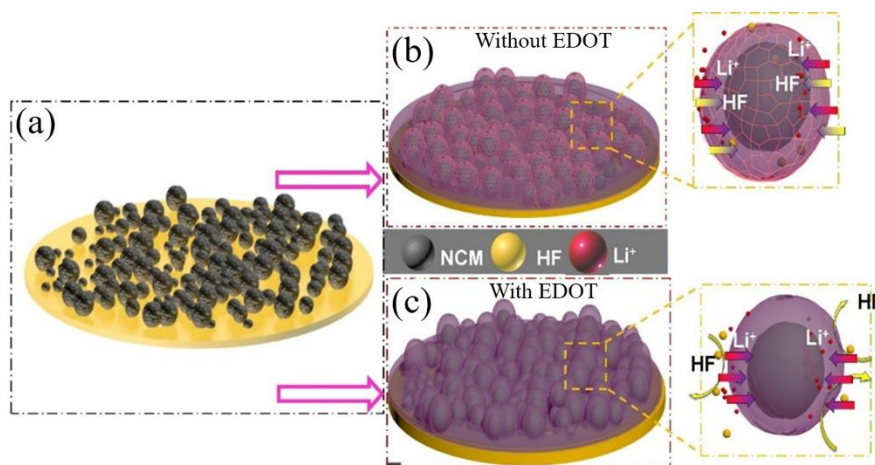
Table 2. Electrochemical data of $\text{LiNi}_{0.8}\text{Co}_{0.1}\text{Mn}_{0.1}\text{O}_2/\text{Li}$ half battery in different electrolytes.

Samples	Initial discharge capacity ($\text{mAh}\cdot\text{g}^{-1}$)	100 th discharge capacity ($\text{mAh}\cdot\text{g}^{-1}$)	Capacity retention after 100 cycles (%)
Blank	185.38	148.57	80.1%
E1	183.97	165.88	90.2%
E2	181.63	169.65	93.4%
E3	181.41	163.28	90.0%

We compared the overcharge potential and cycling performance of similar materials. The relevant comparison data is shown in the Table 3. It is noted that the EDOT as an anti-overcharge additive for NCM811 lithium-ion batteries can exhibit significant enhancement on anti-overcharge protection and cycling performance. It is also believed to the decomposition of EDOT and the formation of the oxidation products on the surface of the positive electrodes, and this leads to the observed improved cycling stability of $\text{Li}/\text{LiNi}_{0.8}\text{Co}_{0.1}\text{Mn}_{0.1}\text{O}_2$ cells at elevated potentials.

Table 3. The comparison with the overcharge potential and cycling performance of similar anti-overcharge additives for LIBs

Additives	Overcharge potential	Cycling performance
Resorcinol bis (diphenyl phosphate)[28]	3.0-4.5 V	1 C, 100 cycle, 86.2%
Lithium difluorophosphate[29]	3.0-4.5 V	1 C, 250 cycle, 89%
Lithium difluorophosphate[30]	3.0-4.5 V	1C, 100 cycle, 78.2%
3,3,3-trifluoropropanoate[31]	3.0-4.6 V	0.2C, 100cycle , 76.1%
3- (Phenylsulfonyl) propionitrile[32]	3.0-4.4 V	0.5C, 200 cycle, 92.5%
3,4-ethylenedioxythiophene (this work)	2.8-4.7 V	0.5C, 100cycle, 93.4%

**Figure 6.** Schematic illustration of the overcharge/discharge process of $\text{LiNi}_{0.8}\text{Co}_{0.1}\text{Mn}_{0.1}\text{O}_2$ electrode:(a) before overcharged; (b) without EDOT; (c) with EDOT.

3.5 Morphological analysis

To further investigate the overcharge protection effect of EDOT on the LIBs with $\text{LiNi}_{0.8}\text{Co}_{0.1}\text{Mn}_{0.1}\text{O}_2$ as the positive electrode material, the SEM images of the cathode electrode sheets before and after overcharged are shown in Fig. 7. Fig. 7(a) shows the SEM image of the fresh positive materials, which is uniformly distributed with sphere structure. After overcharged, the surface of the sample Blank is distributed with loose particles (Fig. 7(b)). While there is little difference in cycled material between EDOT-containing and Blank electrolytes, and the surface of the other three samples after adding EDOT are covered with some dense polymer (Fig. 7(c-e)). This is due to the irreversible reaction of oxidative polymerization of EDOT when the batteries undergo overcharging. The dense substance of the reaction products can effectively increase the interface resistance and block off the rise of voltage. Furthermore, it can effectively preserve the active materials crystal structure.

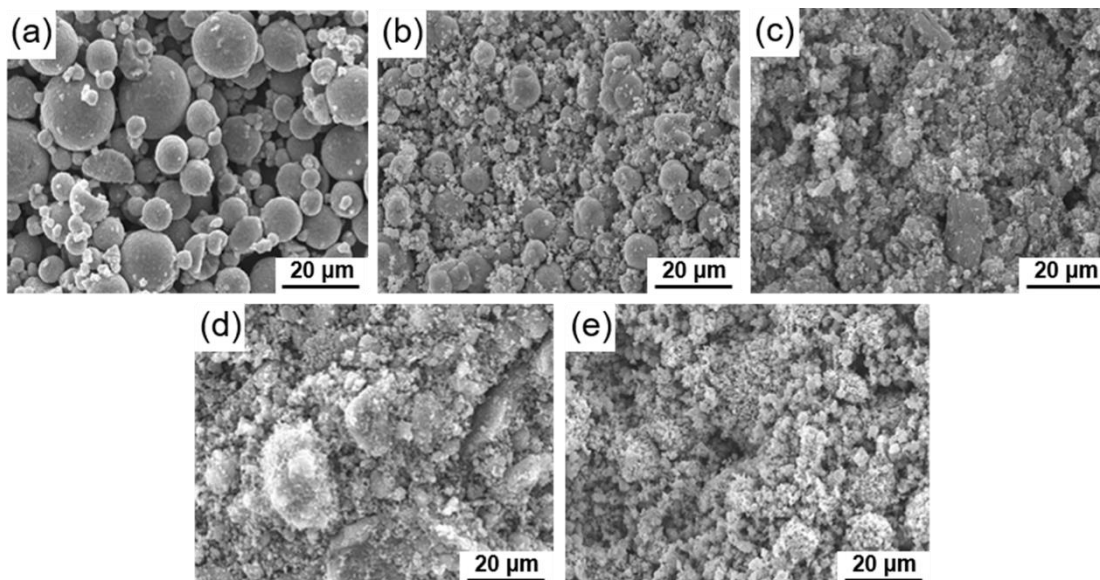


Figure 7. SEM images of $\text{LiNi}_{0.8}\text{Co}_{0.1}\text{Mn}_{0.1}\text{O}_2$ electrodes before (a) and after overcharged with different samples (b)blank, (c) E1, (d) E2, (e) E3.

4. CONCLUSION

In this work, 3,4-ethylenedioxythiophene is successfully introduced to improve the anti-over charged and high voltage electrochemical performance of NCM811 positive materials. Importantly, EDOT can be polymerized at 4.4 V (vs. Li/Li^+) to consume excess charging current, and resulting in a blocking effect for the oxidation of the electrodes and electrolyte. Moreover, the presence of 1.0 wt.% of EDOT results in promising capacity retention after 100 cycles under a high cutoff voltage of 4.7 V. The LSV, EIS and SEM analysis also indicate that EDOT is effective to protect its integrity of primary morphology of NCM811 electrodes. This work provides a reference to develop anti-overcharge additive for Ni-rich positive materials of lithium ion batteries.

ACKNOWLEDGEMENTS

Financial support from National Natural Science Foundation of China (No. 51601081 and 51801086) are gratefully acknowledged.

References

1. Y.N. Zhang, P. Dong, M.Y. Zhang, X.L. Sun, X.H. Yu, J.J. Song, Q. Meng, X. Li and Y.J. Zhang, *J. Appl. Electrochem.*, 48 (2018) 135-145.
2. G.D. Zhang, Y.H. Shi, H.R. Wang, L.L. Jiang, X.D. Yu, S.Y. Jing, S.X. Xing and P. Tsiakaras, *J. Power Sources*, 416 (2019) 118-124.
3. G.R. Zhang, Y.X. Xiang, L.F. Xu, H. Luo, B.L. Wang, Y. Liu, X. Han, W.M. Zhao, S.J. Chen, H.L. Chen, Q.B. Zhang, T. Zhu and Y. Yang, *Adv. Energy Mater.*, 8 (2018) 1801718.
4. Y.J. Bi, W.C. Yang, R. Du, J.J. Zhou, M. Liu, Y. Liu and D.Y. Wang, *J. Power Sources*, 283 (2015) 211-218.
5. L.W. Liang, G.R. Hu, F. Jiang and Y.B. Cao, *J. Alloy. Compd.*, 657 (2016) 570-581.
6. K. Meng, Z.X. Wang, H.J. Guo, X.H. Li and D. Wang, *Electrochim. Acta*, 211 (2016) 822-831.

7. T. Li, X.H. Li, Z.X. Wang and H.J. Guo, *J. Power Sources*, 342 (2017) 495-503.
8. Y. Liu, D.D. Sun, J.J. Zhou, Y.P. Qin, D.Y. Wang and B.K. Guo, *ACS Appl. Mater. Inter.*, 10 (2018) 11305-11310.
9. J.W. Wen, D.W. Zhang, C.H. Chen, C.X. Ding, Y. Yu and J. Maier, *J. Power Sources*, 264 (2014) 155-160.
10. M.X. Dong, Z.X. Wang, H.K. Li, H.J. Guo, X.H. Li, K. Shih and J.X. Wang, *ACS Sustain. Chem. Eng.*, 5 (2017) 10199-10205.
11. R. Du, Y.J. Bi, W.C. Yang, Z. Peng, M. Liu, Y. Liu, B.M. Wu, B.C. Yang, F. Ding and D.Y. Wang, *Ceram. Int.*, 41 (2015) 7133-7139.
12. X.H. Xiong, Z.X. Wang, X. Yin, H.J. Guo and X.H. Li, *Mater. Lett.*, 110 (2013) 4-9.
13. S. Chen, T. He, Y.F. Su, Y. Lu, L.Y. Bao, Q.Y. Zhang, J. Wang, R.J. Chen and F. Wu, *ACS Appl. Mater. Inter.*, 9 (2017) 29732-29743.
14. C.Y. Zhu, J.X. Liu, X.H. Yu, Y.J. Zhang, X.D. Jiang, P. Dong, and Y.N. Zhang, *Int. J. Electrochem. Sci.*, 14 (2019) 4571-4579.
15. X.Z. Zheng, T. Huang, Y. Pan, W.G. Wang, G.H. Fang, K.N. Ding and M.X. Wu, *ACS Appl. Mater. Inter.*, 9 (2017) 18758-18765.
16. L.F. Xiao, X.P. Ai, Y.L. Cao and H.X. Yang, *Electrochim. Acta*, 49 (2004) 4189.
17. D.N. Zhao, P. Wang, Q.P. Zhao, S.Y. Li and Z.F. Zhou, *Energy Technol-GER*, 12 (2018) 2450-2460.
18. S.H. Ju, I.-S. Kang, Y.-S. Lee, W.-K. Shin, S. Kim, K. Shin and D.-W. Kim, *ACS Appl. Mater. Inter.*, 6 (2014) 2546-2552.
19. J.-M. Kim, H.-S. Park, J.-H. Park, T.-H. Kim, H.-K. Song and S.-Y. Lee, *ACS Appl. Mater. Inter.*, 6 (2014) 12789-12797.
20. B. Zhang, P.Y. Dong, H. Tong, Y.Y. Yao, J.C. Zheng, W.J. Yu, J.F. Zhang and D.W. Chu, *J. Alloy. Compd.*, 706 (2017) 198-204.
21. Y.N. Zhang, Y.J. Zhang, J. Rong, J.H. Wu, P. Dong, M.L. Xu, J. Feng and C.D. Gu, *J. Alloy. Compd.*, 795 (2019) 177-186.
22. Y.N. Zhang, P. Dong, J.B. Zhao, X. Li and Y.J. Zhang, *Ceram. Int.*, 45 (2019) 11382-11387.
23. G.G. Amatucci, J.M. Tarascon and L.C. Klein, *Solid State Ionics*, 83 (1996) 167-173.
24. S.-U. Woo, B.-C. Park, C. S. Yoon, S.-T. Myung, Jai Prakash and Y.-K. Sun, *J. Electrochem. Soc.*, 154 (2007) A649-A655.
25. B. Zhao, J. Si, C.H. Cao, J. Zhang, B.J. Xia, J.W. Xie, B.B. Li and Y. Jiang, *Solid State Ionics*, 339 (2019) 114998.
26. U.H. Kim, D.W. Jun, K.J. Park, Q. Zhang, P. Kaghazchi, D. Aurbach, D.T. Major, G. Goobes, M. Dixit, N. Leifer, C.M. Wang, P. Yan, D. Ahn, K.H. Kim, C. S. Yoon and Y.K. Sun, *Energy Environ. Sci.*, 11 (2018) 1271-1279.
27. P. Arora, R.E. White and M. Doyle, *J. Electrochem. Soc.*, 145(1998) 3647-3667.
28. J.K. Feng and L. Li, *J. Power Sources*, 243 (2013) 29-32.
29. J.W. Chen, L.D. Xiang, X.R. Yang, X. Liu, T.J. Li and W.S. Li, *Electrochim. Acta*, 290 (2018) 568-576.
30. C.Y. Wang, L. Y, W.Z. Fan, J.W. Liu, L.Z. Ouyang, L.C. Yang and M. Zhu, *ACS Appl. Energy Mater.*, 6 (2018) 2647-2656.
31. X.Z. Zheng, T. Huang, Y. Pan, W.G. Wang, G.H. Fang, K.N. Ding and M.X. Wu, *ACS Appl. Mater. Inter.*, 9 (2017) 18758-18765.
32. X.X. Zuo, X. Deng, X.D. Ma, J.H. Wu, H.Y. Liang and J.M. Nan, *J. Mater. Chem. A*, 6 (2018) 14725-14733.